

Václav Kučera; Andrea Zivčáková

Discontinuous Galerkin method for a 2D nonlocal flocking model

In: Jan Chleboun and Pavel Kůs and Petr Příkryl and Karel Segeth and Jakub Šístek and Tomáš Vejchodský (eds.): Programs and Algorithms of Numerical Mathematics, Proceedings of Seminar. Janov nad Nisou, June 19-24, 2016. Institute of Mathematics CAS, Prague, 2017. pp. 63–72.

Persistent URL: <http://dml.cz/dmlcz/702999>

Terms of use:

© Institute of Mathematics CAS, 2017

Institute of Mathematics of the Czech Academy of Sciences provides access to digitized documents strictly for personal use. Each copy of any part of this document must contain these *Terms of use*.



This document has been digitized, optimized for electronic delivery and stamped with digital signature within the project *DML-CZ: The Czech Digital Mathematics Library*
<http://dml.cz>

DISCONTINUOUS GALERKIN METHOD FOR A 2D NONLOCAL FLOCKING MODEL

Václav Kučera, Andrea Živčáková

Charles University in Prague, Faculty of Mathematics and Physics
Sokolovská 83, 186 75 Praha, Czech Republic
kucera@karlin.mff.cuni.cz, zivcakova@karlin.mff.cuni.cz

Abstract: We present our work on the numerical solution of a continuum model of flocking dynamics in two spatial dimensions. The model consists of the compressible Euler equations with a nonlinear nonlocal term which requires special treatment. We use a semi-implicit discontinuous Galerkin scheme, which proves to be efficient enough to produce results in 2D in reasonable time. This work is a direct extension of the authors' previous work in 1D.

Keywords: discontinuous Galerkin method, semi-implicit time discretization, nonlocal problems, flocking dynamics

MSC: 65M60, 35Q92, 35Q35

1. Introduction

The study of emergent collective behavior and phenomena in natural and artificial systems is a very popular and diverse field, cf. [1], [9], [10] for an overview. One of the topics of interest is that of global coordination of behavior seen in flocks of birds or other similar self-propelled entities. The study of such problems leads to descriptions on various levels (particle, kinetic and hydrodynamic) and various models of the underlying behavior of the individuals, cf. [10]. The paper [7] deals with the derivation of a hydrodynamic limit of a certain modification of the famous Cucker-Smale model [2], [3]. The resulting partial differential equation consists of the compressible Euler equation of gas dynamics, with an additional nonlinear nonlocal term. The presence of this term leads to difficulties in constructing an efficient numerical scheme, which would produce results in a reasonable time (e.g. hours) even on very coarse grids in 1D, cf. [7].

This short note presents results obtained using a two-dimensional version of the 1D numerical scheme presented in [8]. The scheme is based on a semi-implicit time discretization of the discontinuous Galerkin (DG) scheme from [6] originally applied to the compressible Euler equations. In [8], the semi-implicit scheme was extended to include the nonlinear and nonlocal interaction terms of the considered flocking

model in an efficient way. Here we show how to perform the discretization in the 2D case and present numerical experiments obtained with the resulting scheme.

2. Mathematical model

We consider the hydrodynamic model of flocking derived in [7] as a macroscopic limit of a modification of the Cucker-Smale model [2], [3].

Let $\Omega \subset \mathbb{R}^d$, $d = 1, 2$, be a bounded domain and $0 < L < +\infty$ is the length of a time interval. We set $Q_L := \Omega \times (0, L)$. We treat the following problem: Find $\rho, E : Q_L \rightarrow \mathbb{R}$, $\mathbf{u} = (u_1, \dots, u_d) : Q_L \rightarrow \mathbb{R}^d$ such that

$$\begin{aligned} \frac{\partial \rho}{\partial t} + \operatorname{div}(\rho \mathbf{u}) &= 0, \\ \frac{\partial(\rho \mathbf{u})}{\partial t} + \operatorname{div}(\rho \mathbf{u} \otimes \mathbf{u}) + \nabla p &= \lambda \mathcal{A}(\rho, \mathbf{u}), \\ \frac{\partial E}{\partial t} + \operatorname{div}\left(\mathbf{u}(E + p)\right) &= \lambda \mathcal{B}(\rho, \mathbf{u}, E), \end{aligned} \quad (1)$$

where ρ denotes the density, E energy, p pressure and \mathbf{u} velocity. The relations between E and p are

$$E = \rho \left(\frac{T}{\gamma - 1} + \frac{|\mathbf{u}|^2}{2} \right), \quad p = \rho T, \quad (2)$$

where $\gamma = \frac{d+2}{d}$ is the adiabatic constant and T temperature. These quantities describe the macroscopic behavior of agents behaving according to the microscopic model considered in [7]. In this context, the basic variables must be interpreted in the Boltzmannian framework - e.g. momentum $\rho \mathbf{u}$ and temperature T are the first and second moments of the density distribution function $f(x, \mathbf{v}, t)$ in the corresponding kinetic (mesoscopic) model from which the hydrodynamic model (1) is derived, cf. [7].

The right-hand side functions \mathcal{A} and \mathcal{B} are given by

$$\begin{aligned} \mathcal{A}(\rho, \mathbf{u})(\mathbf{x}, t) &= \int_{\mathbb{R}^d} \tilde{\mathbf{n}}(\mathbf{x}, \mathbf{y}) b(\mathbf{x}, \mathbf{y}) \left(\mathbf{u}(\mathbf{y}, t) - \mathbf{u}(\mathbf{x}, t) \right) \cdot \tilde{\mathbf{n}}(\mathbf{x}, \mathbf{y}) \rho(\mathbf{x}, t) \rho(\mathbf{y}, t) d\mathbf{y}, \\ \mathcal{B}(\rho, \mathbf{u}, E)(\mathbf{x}, t) &= \int_{\mathbb{R}^d} b(\mathbf{x}, \mathbf{y}) \rho(\mathbf{x}, t) \left(\rho(\mathbf{y}, t) \tilde{\mathbf{n}}(\mathbf{x}, \mathbf{y}) \cdot \mathbf{u}(\mathbf{x}, t) \tilde{\mathbf{n}}(\mathbf{x}, \mathbf{y}) \cdot \mathbf{u}(\mathbf{y}, t) \right. \\ &\quad \left. - \frac{2}{d} E(\mathbf{y}, t) \right) d\mathbf{y}, \end{aligned} \quad (3)$$

where

$$b(\mathbf{x}, \mathbf{y}) = \frac{\lambda K}{(\lambda + |\mathbf{x} - \mathbf{y}|^2)^{\beta+1}}, \quad \tilde{\mathbf{n}}(\mathbf{x}, \mathbf{y}) = (\tilde{n}_1, \dots, \tilde{n}_d) = \frac{\mathbf{x} - \mathbf{y}}{|\mathbf{x} - \mathbf{y}|}, \quad (4)$$

and $K, \lambda > 0$ and $\beta \geq 0$ are given constants.

By omitting the right-hand side terms \mathcal{A}, \mathcal{B} from (1), we obtain the compressible Euler equations. In this light, we rewrite system (1) as a system of conservation laws with a right-hand side source terms:

$$\frac{\partial \mathbf{w}}{\partial t} + \sum_{s=1}^d \frac{\partial \mathbf{f}_s(\mathbf{w})}{\partial x_s} = \mathbf{g}(\mathbf{w}) \quad \text{in } Q_L, \quad (5)$$

where

$$\begin{aligned} \mathbf{w} &= (w_1, \dots, w_{d+2}) = (\rho, \rho u_1, \dots, \rho u_d, E)^\top \in \mathbb{R}^{d+2}, \\ \mathbf{f}_s(\mathbf{w}) &= (\rho u_s, \rho u_s u_1 + \delta_{s1}, \rho u_s u_2 + \delta_{s2} p, (E + p) u_s)^\top, \\ \mathbf{g}(\mathbf{w}) &= (0, \mathcal{A}(\mathbf{w}), \mathcal{B}(\mathbf{w}))^\top = (0, \mathcal{A}_1(\mathbf{w}), \dots, \mathcal{A}_d(\mathbf{w}), \mathcal{B}(\mathbf{w}))^\top. \end{aligned} \quad (6)$$

Here δ is the Kronecker delta. The vector-valued function \mathbf{w} is called the *state vector* and the functions $\mathbf{f}_s, s = 1, \dots, d$, are the *Euler fluxes*. In (5), we write the right-hand side terms \mathcal{A}, \mathcal{B} as functions of the state vector \mathbf{w} , although in (1), they are written terms of the nonconservative variables. Expressing \mathcal{A}, \mathcal{B} in \mathbf{w} in a suitable way is a key ingredient in our scheme and will be described in detail in Section 3.4.

The resulting system is equipped with the initial condition $\mathbf{w}(x, 0) = \mathbf{w}^0(x)$ for $x \in \Omega$. In 1D case we use periodic boundary conditions and in 2D we chose conditions corresponding to solid impermeable walls, i.e. $\mathbf{u} \cdot \mathbf{n} = 0$ on $\partial\Omega$.

Euler fluxes are homogeneous functions, which implies the useful relations

$$\mathbf{f}_s(\mathbf{w}) = \mathbb{A}_s(\mathbf{w})\mathbf{w}, \quad \mathbb{A}_s = \frac{D\mathbf{f}_s}{D\mathbf{w}}, \quad s = 1, \dots, d. \quad (7)$$

Furthermore, the Euler flux is *diagonally hyperbolic*: The matrix

$$\mathbb{P}(\mathbf{w}, \bar{\mathbf{n}}) := \sum_{s=1}^d \mathbb{A}_s(\mathbf{w}) \bar{n}_s \quad (8)$$

is diagonalizable with real eigenvalues, where $\bar{\mathbf{n}} = (\bar{n}_1, \dots, \bar{n}_d)$ denotes a unit vector. This means there exists $\mathbb{T}(\mathbf{w}, \bar{\mathbf{n}}) \in \mathbb{R}^{d+2, d+2}$ and a diagonal matrix $\mathbb{D}(\mathbf{w}, \bar{\mathbf{n}}) \in \mathbb{R}^{d+2, d+2}$ such that

$$\mathbb{P}(\mathbf{w}, \bar{\mathbf{n}}) = \mathbb{T} \mathbb{D} \mathbb{T}^{-1}, \quad \text{where } \mathbb{D}(\mathbf{w}, \bar{\mathbf{n}}) = \text{diag}(\lambda_1, \lambda_2, \dots, \lambda_{d+2}). \quad (9)$$

3. Discretization

Let \mathcal{T}_h be a triangulation of Ω , i.e. a partition of $\bar{\Omega}$ into a finite number of closed simplices with mutually disjoint interiors. By \mathcal{F}_h we denote the system of all faces (i.e. nodes in 1D) of \mathcal{T}_h . For each $\Gamma \in \mathcal{F}_h$ we choose and fix a unit normal \mathbf{n}_Γ , which, for $\Gamma \subset \partial\Omega$ has the same orientation as the outer normal to Ω .

For each *interior* face $\Gamma \in \mathcal{F}_h$ there exist two neighbours $K_\Gamma^{(L)}, K_\Gamma^{(R)} \in \mathcal{T}_h$ such that $\Gamma = K_\Gamma^{(L)} \cap K_\Gamma^{(R)}$. We use the convention that \mathbf{n}_Γ is the outer normal to the element $K_\Gamma^{(L)}$. For a function v piecewise defined on \mathcal{T}_h and $\Gamma \in \mathcal{F}_h$ we introduce:

$$\begin{aligned} v|_\Gamma^{(L)} &= \text{the trace of } v|_{K_\Gamma^{(L)}} \text{ on } \Gamma, & v|_\Gamma^{(R)} &= \text{the trace of } v|_{K_\Gamma^{(R)}} \text{ on } \Gamma, \\ \langle v \rangle_\Gamma &= \frac{1}{2}(v|_\Gamma^{(L)} + v|_\Gamma^{(R)}), & [v]_\Gamma &= v|_\Gamma^{(L)} - v|_\Gamma^{(R)}, \end{aligned}$$

where on $\partial\Omega$, we define $v|_\Gamma^{(R)}$ using the boundary conditions as in [6].

If $[\cdot]_\Gamma$ and $\langle \cdot \rangle_\Gamma$ appear in an integral of the form $\int_\Gamma \dots dS$, we omit the subscript Γ and write simply $[\cdot]$ and $\langle \cdot \rangle$. We shall use the following notation:

$$\int_{\mathcal{F}_h} F(x) dS = \sum_{\Gamma \in \mathcal{F}_h} \int_\Gamma F(x) dS$$

and similarly for $\int_{\partial K} F(x) dS$ etc.

Let $m \geq 0$ be an integer. The approximate solution will be sought in the space of discontinuous piecewise polynomial functions

$$\mathbf{S}_h := [S_h]^{d+2}, \text{ where } S_h = \{v; v|_K \in P^m(K), \forall K \in \mathcal{T}_h\}.$$

Here $P^m(K)$ denotes the space of all polynomials on K of degree $\leq m$.

3.1. Discontinuous Galerkin space semidiscretization

Similarly as in [6] in the case of the Euler equations and in [8] in the case of the 1D flocking model, we multiply (5) by a test function $\varphi \in \mathbf{S}_h$, integrate over $K \in \mathcal{T}_h$ and apply integration by parts in the convective terms and rearrange:

$$\int_\Omega \frac{\partial \mathbf{w}}{\partial t} \cdot \varphi d\mathbf{x} + \sum_{s=1}^d \left(\int_{\mathcal{F}_h} \mathbf{f}_s(\mathbf{w}) n_s \cdot [\varphi] dS - \sum_{K \in \mathcal{T}_h} \int_K \mathbf{f}_s(\mathbf{w}) \cdot \frac{\partial \varphi}{\partial x_s} d\mathbf{x} \right) = \int_\Omega \mathbf{g}(\mathbf{w}) \cdot \varphi d\mathbf{x}. \quad (10)$$

Since \mathbf{w} is approximated by a discontinuous function, we use a *numerical flux* $\mathbf{H}_s(\mathbf{w}^{(L)}, \mathbf{w}^{(R)}, \mathbf{n})$ in the boundary integral term:

$$\int_{\mathcal{F}_h} \sum_{s=1}^d \mathbf{f}_s(\mathbf{w}) n_s \cdot [\varphi] dS \approx \int_{\mathcal{F}_h} \mathbf{H}(\mathbf{w}^{(L)}, \mathbf{w}^{(R)}, \mathbf{n}) \cdot [\varphi] dS. \quad (11)$$

Specifically, in our implementation we used the Vijayasundaram numerical flux, cf. Section 3.2.

Now we can define the following forms defined for $\mathbf{w}, \varphi \in H^1(\Omega, \mathcal{T}_h)$.

Convective form:

$$b_h(\mathbf{w}, \varphi) = \int_{\mathcal{F}_h} \mathbf{H}(\mathbf{w}^{(L)}, \mathbf{w}^{(R)}, \mathbf{n}) \cdot [\varphi] dS - \sum_{K \in \mathcal{T}_h} \int_K \sum_{s=1}^d \mathbf{f}_s(\mathbf{w}) \cdot \frac{\partial \varphi}{\partial x_s} d\mathbf{x}.$$

Right-hand side source form:

$$l_h(\mathbf{w}, \boldsymbol{\varphi}) = - \int_{\Omega} \mathbf{g}(\mathbf{w}) \cdot \boldsymbol{\varphi} \, d\mathbf{x}.$$

Definition 1. We say that $\mathbf{w}_h \in C^1([0, T]; \mathcal{S}_h)$ is a DG solution of problem (5) if $\mathbf{w}_h(0) = \mathbf{w}_h^0$, an \mathcal{S}_h -approximation of the initial condition \mathbf{w}^0 and

$$\frac{d}{dt}(\mathbf{w}_h(t), \boldsymbol{\varphi}_h) + b_h(\mathbf{w}_h(t), \boldsymbol{\varphi}_h) + l_h(\mathbf{w}_h(t), \boldsymbol{\varphi}_h) = 0 \quad \forall \boldsymbol{\varphi}_h \in \mathcal{S}_h, \quad \forall t \in (0, T). \quad (12)$$

3.2. Numerical flux

The choice of the numerical flux is a very important topic in the finite volume and DG schemes. We use the *Vijayasundaram* numerical flux, cf. [11], which is suitable for our semi-implicit time discretization. This numerical flux is based on the flux vector splitting concept, and can be viewed as an extension of the upwind numerical flux to systems of equations. We use the diagonal hyperbolicity (9) and define the *positive* and *negative* parts of matrix \mathbb{P} :

$$\mathbb{P}^{\pm}(\mathbf{w}, \bar{\mathbf{n}}) = \mathbb{T}(\mathbf{w}, \bar{\mathbf{n}}) \mathbb{D}^{\pm}(\mathbf{w}, \bar{\mathbf{n}}) \mathbb{T}^{-1}(\mathbf{w}, \bar{\mathbf{n}}), \quad \mathbb{D}^{\pm}(\mathbf{w}, \bar{\mathbf{n}}) = \text{diag}(\lambda_1^{\pm}, \lambda_2^{\pm}, \dots, \lambda_{d+2}^{\pm}), \quad (13)$$

where $\lambda^+ = \max\{0, \lambda\}$, $\lambda^- = \min\{0, \lambda\}$. Then $\mathbb{P}(\mathbf{w}, \bar{\mathbf{n}}) = \mathbb{P}^+(\mathbf{w}, \bar{\mathbf{n}}) + \mathbb{P}^-(\mathbf{w}, \bar{\mathbf{n}})$ and we can define the Vijayasundaram numerical flux as

$$\mathbf{H}_{VS}(\mathbf{w}^{(L)}, \mathbf{w}^{(R)}, \bar{\mathbf{n}}) = \mathbb{P}^+ \left(\frac{\mathbf{w}^{(L)} + \mathbf{w}^{(R)}}{2}, \bar{\mathbf{n}} \right) \mathbf{w}^{(L)} + \mathbb{P}^- \left(\frac{\mathbf{w}^{(L)} + \mathbf{w}^{(R)}}{2}, \bar{\mathbf{n}} \right) \mathbf{w}^{(R)}. \quad (14)$$

Explicit formulas for \mathbb{P} , \mathbb{T} , \mathbb{T}^{-1} and \mathbb{D} can be found e.g. in [5].

3.3. Time discretization

After choosing some basis of the space \mathcal{S}_h , equation (12) represents a system of nonlinear ordinary differential equations, which must be discretized with respect to time. Due to severe time step restrictions caused by the nonlocality and nonlinearity of system (1), we want to avoid using an explicit scheme. However an implicit time discretization is also very expensive due to its nonlinearity. Therefore we choose the semi-implicit scheme of [6] as a basis and apply it to our problem.

Let $0 = t_0 < t_1 < t_2 < \dots$ be a partition of time interval $[0, L]$ and define $\tau_k = t_{k+1} - t_k$. We use a first order backward difference approximation for the time derivative, i.e.

$$\frac{\partial \mathbf{w}_h(t_{k+1})}{\partial t} \approx \frac{\mathbf{w}_h^{k+1} - \mathbf{w}_h^k}{\tau_k},$$

where $\mathbf{w}_h^k \approx \mathbf{w}_h(t_k)$ and $\mathbf{w}_h^k \in \mathcal{S}_h$. The backward Euler scheme reads

$$\left(\frac{\mathbf{w}_h^{k+1} - \mathbf{w}_h^k}{\tau_k}, \boldsymbol{\varphi}_h \right) + b_h(\mathbf{w}_h^{k+1}, \boldsymbol{\varphi}_h) + l_h(\mathbf{w}_h^{k+1}, \boldsymbol{\varphi}_h) = 0 \quad \forall \boldsymbol{\varphi}_h \in \mathcal{S}_h, \quad (15)$$

for all $k = 0, 1, \dots$. Equation (15) is nonlinear with respect to the unknown \mathbf{w}_h^{k+1} , therefore we linearize the scheme.

In the convective form, we linearize the interior terms using the homogeneity (7) as $\mathbf{f}_s(\mathbf{w}_h^{k+1}) \approx \mathbb{A}_s(\mathbf{w}_h^k)\mathbf{w}_h^{k+1}$. In the boundary terms, we use the Vijayasundaram numerical flux (14) and linearize by taking the matrices \mathbb{P}_s^+ and \mathbb{P}_s^- from the previous time level. Thus we get the linearize convective form

$$\begin{aligned} \tilde{b}_h(\mathbf{w}_h^k, \mathbf{w}_h^{k+1}, \boldsymbol{\varphi}_h) &= - \sum_{K \in \mathcal{T}_h} \int_K \sum_{s=1}^d \mathbb{A}_s(\mathbf{w}_h^k) \mathbf{w}_h^{k+1} \cdot \frac{\partial \boldsymbol{\varphi}_h}{\partial x_s} \, d\mathbf{x} \\ &+ \int_{\mathcal{F}_h} \left(\mathbb{P}^+(\langle \mathbf{w}_h^k, \mathbf{n} \rangle) \mathbf{w}_h^{k+1, (L)} + \mathbb{P}^-(\langle \mathbf{w}_h^k, \mathbf{n} \rangle) \mathbf{w}_h^{k+1, (R)} \right) \cdot [\boldsymbol{\varphi}_h] \, dS. \end{aligned} \quad (16)$$

In the source terms we again linearize them to obtain the approximation $l_h(\mathbf{w}_h^{k+1}, \boldsymbol{\varphi}_h) \approx \tilde{l}_h(\mathbf{w}_h^k, \mathbf{w}_h^{k+1}, \boldsymbol{\varphi}_h)$, cf. Section 3.4 for details.

Collecting all the considerations, we obtain the following semi-implicit DG scheme:

Definition 2. We say that the sequence $\mathbf{w}_h^k \in \mathcal{S}_h, k = 0, 1, \dots$, is a semi-implicit DG solution of problem (5) if for all $\boldsymbol{\varphi}_h \in S_h$

$$\left(\frac{\mathbf{w}_h^{k+1} - \mathbf{w}_h^k}{\tau_k}, \boldsymbol{\varphi}_h \right) + \tilde{b}_h(\mathbf{w}_h^k, \mathbf{w}_h^{k+1}, \boldsymbol{\varphi}_h) + \tilde{l}_h(\mathbf{w}_h^k, \mathbf{w}_h^{k+1}, \boldsymbol{\varphi}_h) = 0. \quad (17)$$

3.4. Linearization of the source terms l_h

As the 1D case is treated in [8], we demonstrate the linearization of the nonlocal terms only in 2D. First, we rewrite the right-hand side integrals \mathcal{A} and \mathcal{B} in terms of the conservative variables.

$$\begin{aligned} \mathbf{g}(\mathbf{w}(\mathbf{x}, t)) &= \int_{\Omega} \begin{pmatrix} 0 \\ \mathcal{A}_1(\mathbf{w}(\mathbf{x}, t)) \\ \mathcal{A}_2(\mathbf{w}(\mathbf{x}, t)) \\ \mathcal{B}(\mathbf{w}(\mathbf{x}, t)) \end{pmatrix} d\mathbf{y} \\ &= \int_{\Omega} b(\mathbf{x}, \mathbf{y}) \rho(\mathbf{x}, t) \begin{pmatrix} 0 \\ \tilde{n}_1 \rho(\mathbf{y}, t) (\mathbf{u}(\mathbf{y}, t) - \mathbf{u}(\mathbf{x}, t)) \cdot \tilde{\mathbf{n}}(\mathbf{x}, \mathbf{y}) \\ \tilde{n}_2 \rho(\mathbf{y}, t) (\mathbf{u}(\mathbf{y}, t) - \mathbf{u}(\mathbf{x}, t)) \cdot \tilde{\mathbf{n}}(\mathbf{x}, \mathbf{y}) \\ \rho(\mathbf{y}, t) \mathbf{u}(\mathbf{x}, t) \cdot \tilde{\mathbf{n}}(\mathbf{x}, \mathbf{y}) \mathbf{u}(\mathbf{y}, t) \cdot \tilde{\mathbf{n}}(\mathbf{x}, \mathbf{y}) - E(\mathbf{y}, t) \end{pmatrix} d\mathbf{y} \\ &= \int_{\Omega} b(\mathbf{x}, \mathbf{y}) \mathbb{U}(\mathbf{w}(\mathbf{y}, t)) \mathbf{w}(\mathbf{x}, t) d\mathbf{y}, \end{aligned} \quad (18)$$

where $\mathbb{U}(\mathbf{w}(\mathbf{y}, t))$ is

$$\begin{pmatrix} 0 & 0 & 0 & 0 \\ \tilde{n}_1^2 w_2(\mathbf{y}, t) + \tilde{n}_1 \tilde{n}_2 w_3(\mathbf{y}, t) & -\tilde{n}_1^2 w_1(\mathbf{y}, t) & -\tilde{n}_1 \tilde{n}_2 w_1(\mathbf{y}, t) & 0 \\ \tilde{n}_1 \tilde{n}_2 w_2(\mathbf{y}, t) + \tilde{n}_2^2 w_3(\mathbf{y}, t) & -\tilde{n}_1 \tilde{n}_2 w_1(\mathbf{y}, t) & -\tilde{n}_2^2 w_1(\mathbf{y}, t) & 0 \\ -w_4(\mathbf{y}, t) & \tilde{n}_1 \tilde{n}_2 w_3(\mathbf{y}, t) + \tilde{n}_1^2 w_2(\mathbf{y}, t) & \tilde{n}_1 \tilde{n}_2 w_2(\mathbf{y}, t) + \tilde{n}_2^2 w_3(\mathbf{y}, t) & 0 \end{pmatrix}.$$

Approximating $\mathbf{w}(\mathbf{x}, t) \approx \mathbf{w}_h^{k+1}(\mathbf{x})$ and $\mathbf{w}(\mathbf{y}, t) \approx \mathbf{w}_h^k(\mathbf{y})$ leads to the linearized form

$$\tilde{l}_h(\mathbf{w}_h^k, \mathbf{w}_h^{k+1}, \boldsymbol{\varphi}_h) = - \int_{\Omega} \left(\int_{\Omega} b(\mathbf{x}, \mathbf{y}) \mathbb{U}(\mathbf{w}_h^k(\mathbf{y})) \, d\mathbf{y} \right) \mathbf{w}_h^{k+1}(\mathbf{x}) \cdot \boldsymbol{\varphi}_h(\mathbf{x}) \, d\mathbf{x}. \quad (19)$$

If we use a basis for \mathcal{S}_h consisting of functions whose support is exactly one element, the form (19) does not change the structure of the system matrix, since it contributes only to the block-diagonal. This is important as other expressions than (18) are possible, however they lead to a full system matrix which is undesirable.

We note, that the computation of the source terms (19) is very time consuming due to their nonlocal nature. Even if the basis functions of \mathcal{S}_h are local, in order to evaluate \tilde{l}_h , we must compute the inner integral $\int_{\Omega} b(\mathbf{x}, \mathbf{y}) \mathbb{U}_2(\mathbf{w}_h^k(\mathbf{y})) \, d\mathbf{y}$, which is time consuming due to the slow decay of the function $b(\mathbf{x}, \mathbf{y})$.

3.5. Shock capturing and treatment of vacuum

Numerical experiments from the 1D case show that the solution of (1) typically contains quickly moving shocks and near vacuum states. Often, one observes shocks neighboring a vacuum, even in the stationary case, which is impossible for the Euler equations themselves. The situation is quite similar in 2D. To treat these problems, we include the shock capturing terms of [6]. Furthermore, special attention must be given to the treatment of the occurrence of vacuum - when ρ, p or T are near zero, or even numerically negative due to spurious oscillations in the solution, the matrices $\mathbb{A}, \mathbb{P}^+, \mathbb{P}^-$ are no longer defined and the computation collapses. We therefore use the "postprocessing" approach from [8]. The newly computed state \mathbf{w}_h^k is modified thus: if $\rho < \varepsilon$ or $T < \varepsilon$, then set $\rho := \varepsilon$ or $T := \varepsilon$ and recompute the energy E using relation (2). This defines a new state $\tilde{\mathbf{w}}_h^k$ which is used in (17) instead of \mathbf{w}_h^k to compute \mathbf{w}_h^{k+1} . In our case, we use $\varepsilon := 10^{-5}$. In combination with the shock capturing procedure of [6], this yields a sufficiently robust scheme.

4. Numerical tests

We considered the 2D problem on a unit square. In the first numerical experiment was prescribed the initial density distribution as a Gaussian bump given by $\rho(x, y) = \exp(-10|(x, y) - (0.5, 0.5)|^2)$ with constant temperature $T = 10$ and the velocity distribution $\mathbf{u}(x, y) = (0, 0)$. This is a two-dimensional analogue of the problem solved in [8]. Similarly as in the 1D case, after an initial phase of rapid oscillations, was observed the concentration of the hump. Density plots at chosen time instances are given in Figure 1 (ordered left to right, top to bottom). Due to the concentration of density, the solution converges to a tall "spike", so the graphs are cut of at the same value of 1.1 for clarity.

The second numerical experiment consisted of two neighboring Gaussian bumps, one smaller than the other in magnitude. In this case, the two groups merged into one single "flock", as seen in Figure 2.

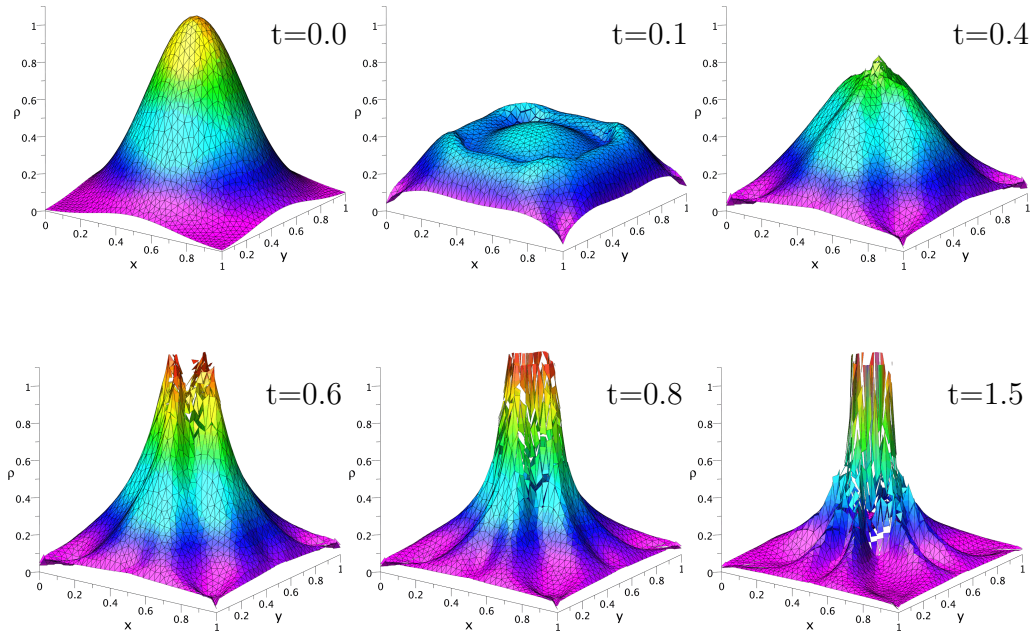


Figure 1: Numerical experiment 1 – density distribution.

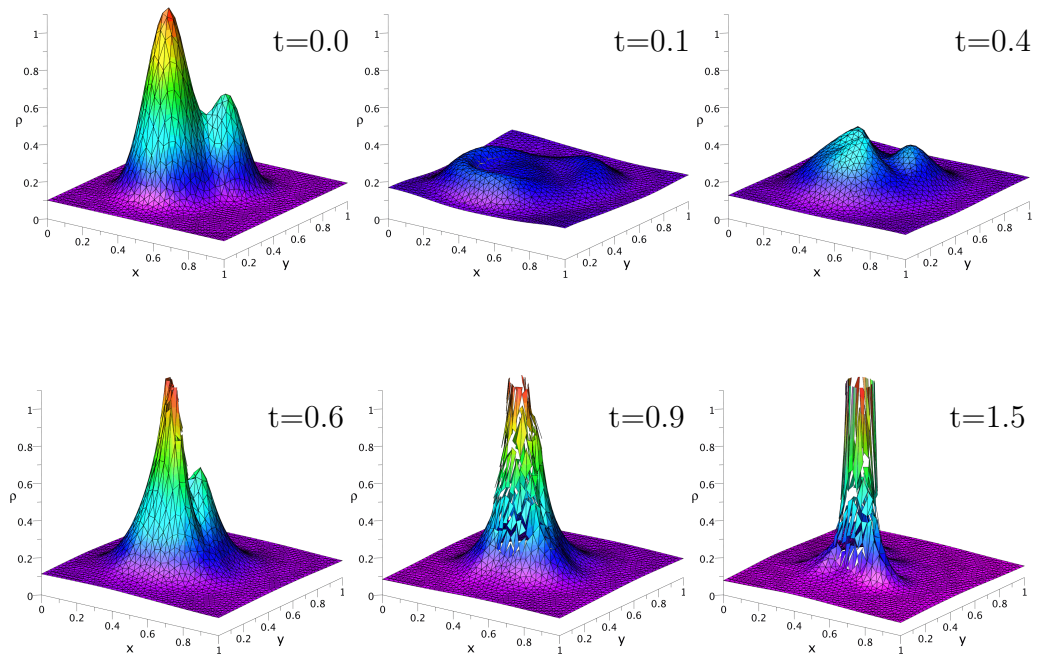


Figure 2: Numerical experiment 2 – density distribution.

We performed both numerical experiments on an unstructured mesh consisting of 3057 element with piecewise linear approximation. The constants needed in (4) were chosen as $K = 10$, $\beta = 0.1$, $\lambda = 1$, following [7].

5. Conclusions

In this paper we have presented a practical application of the discontinuous Galerkin method to nonlocal problems, namely for a complicated nonlinear and non-local version of the compressible Euler equations describing the dynamics of flocks of birds. Straightforward discretizations of the problem are extremely inefficient due to its nonlocal nature and the need to evaluate the nonlocal terms too many times. We shown how to obtain numerical solutions in reasonable time using a very efficient time discretization of the discontinuous Galerkin method.

Acknowledgements

The research of V. Kučera is supported by the Grant No. P201/13/00522S of the Czech Science Foundation. The research of A. Živčáková is supported by the Charles University in Prague, project GA UK No. 758214.

References

- [1] Camazine, S., Deneubourg, J.-L., Franks, N.R., Sneyd, J., Theraulaz, G., and Bonabeau, E.: *Self-organization in biological systems*. Princeton University Press, 2003.
- [2] Cucker, F. and Smale, S.: Emergent behavior in flocks. *IEEE Trans. Automat. Control* **52** (2007), 852–862.
- [3] Cucker, F. and Smale, S.: On the mathematics of emergence. *Japan J. Math.* **2** (2007), 197–227.
- [4] Davis, T.A. and Duff, I.S.: A combined unifrontal/multifrontal method for unsymmetric sparse matrices. *ACM Transact. on Math. Soft.* **25** (1999), 1–19.
- [5] Feistauer, M., Felcman, J., and Straškraba, I.: *Mathematical and computational methods for compressible flow*. Clarendon Press, Oxford, 2003.
- [6] Feistauer, M. and Kučera, V.: On a robust discontinuous Galerkin technique for the solution of compressible flow. *J. Comput. Phys.*, **224** (2007), 208–221.
- [7] Fornasier, M., Haškovec J., and Toscani, G.: Fluid dynamic description of flocking via Povzner-Boltzmann equation. *Physica D* **240** (1) (2011), 21–31.
- [8] Kučera, V. and Živčáková, A.: Numerical solution of a new hydrodynamic model of flocking dynamics. In: *Programs and Algorithms of Numerical Mathematics 17*, pp. 124–129. Institute of Mathematics, CAS, Prague, 2015.

- [9] Muntean, A. and Toschi, F. (Eds.): *Collective dynamics from bacteria to crowds*, Springer, 2014.
- [10] Naldi, G., Pareschi, L., and Toscani, G. (Eds.): *Mathematical modeling of collective behavior in socio-economic and life sciences*, Birkhauser, Boston, 2010.
- [11] Vijayasundaram, G.: Transonic flow simulation using upstream centered scheme of Godunov type in finite elements. *J. Comput. Phys.* **63** (1986), 416–433.